R. Doerner (Herausgeber)
M. Rudolph (Herausgeber)

Selected Topics on Microwave Measurements, Noise in Devices and Circuits, and Transistor Modeling

A Festschrift for Peter Heymann

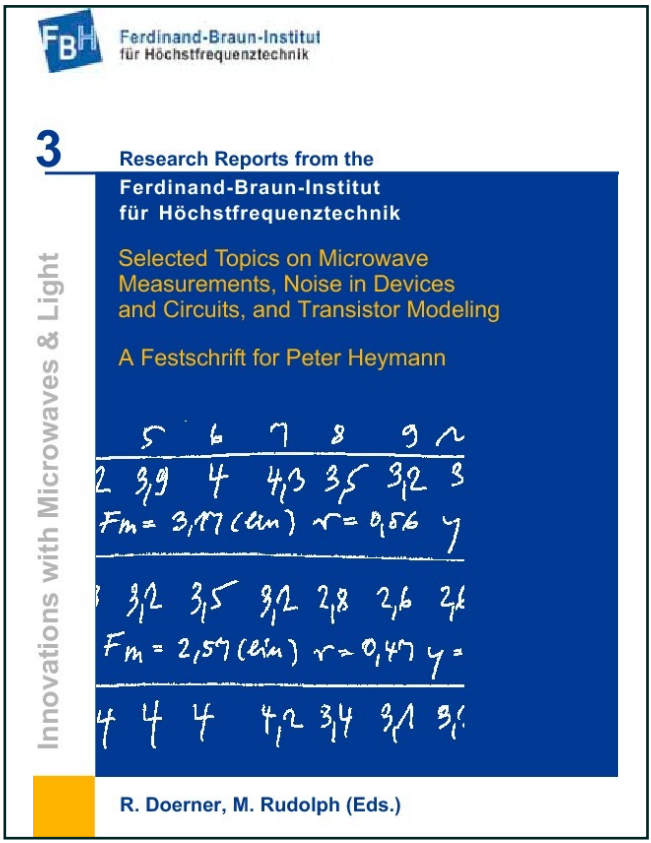

https://cuvillier.de/de/shop/publications/2710

Spectrum Broadening and Fluctuations of Lower Hybrid Waves Observed in the CASTOR Tokamak

F. Žáček, R. Klíma, K. Jakubka, P. Plíšek, S. Nanobashvili*,
P. Pavlo, J. Preinhaelter, J. Stöckel and L. Kryška
Institute of Plasma Physics, Za Slovankou 3, 182 00 Prague 8,
Czech Republic
*Institute of Physics, Tamarashvili 6, 380077 Tbilisi, Georgia

first published in *Plasma Phys. Control. Fusion* 41 (1999) 1221-1230

Abstract

Strong fluctuations of lower hybrid waves (LHW) amplitudes inside the plasma have been observed in experiments with different types of launchers. The fluctuations frequency is much higher than the frequency of plasma density fluctuations. This effect is explained by the presence of plasma fluctuations along the whole ray path. LHW spectrum broadening has been found by means of a double radiofrequency probe. This experimental result supports the assumption of spectral gap filling between the electron velocity distribution function and the spectrum launched into the plasma.

I. Introduction

RECENTLY, measurements of low-power LHW launched into the tokamak CASTOR plasma by several types of quasi-optical grills were performed [1]–[5]. To fulfil requirements of the quasi-optics a relatively high frequency $f = 9.3\,\mathrm{GHz}$ has been chosen lying in the upper part of the LHW band. The main goal of these investigations at low power level has not been a manifestation of the current generation itself, but a direct proof whether or not such quasi-optical system is able to excite LHW in tokamak plasma. For this purpose, i.e. for the measurement of $N_{\|}$ inside the plasma, a double radiofrequency (RF) probe movable through the whole small tokamak cross section has been developed and installed in CASTOR. Here, $N_{\|} = (c/2\pi f)k_{\|}$ is the index of refractivity of the launched LHW, c is the velocity of light and k is the wavevector. The subscript $\|$ denotes the component of the corresponding quantity in the direction of the magnetic field. Two indications that the wave observed is the LH wave have been gained:

(a) a region of enhanced RF field has been found in the cross section where ray tracing predicts an occurrence of LH conus [1];

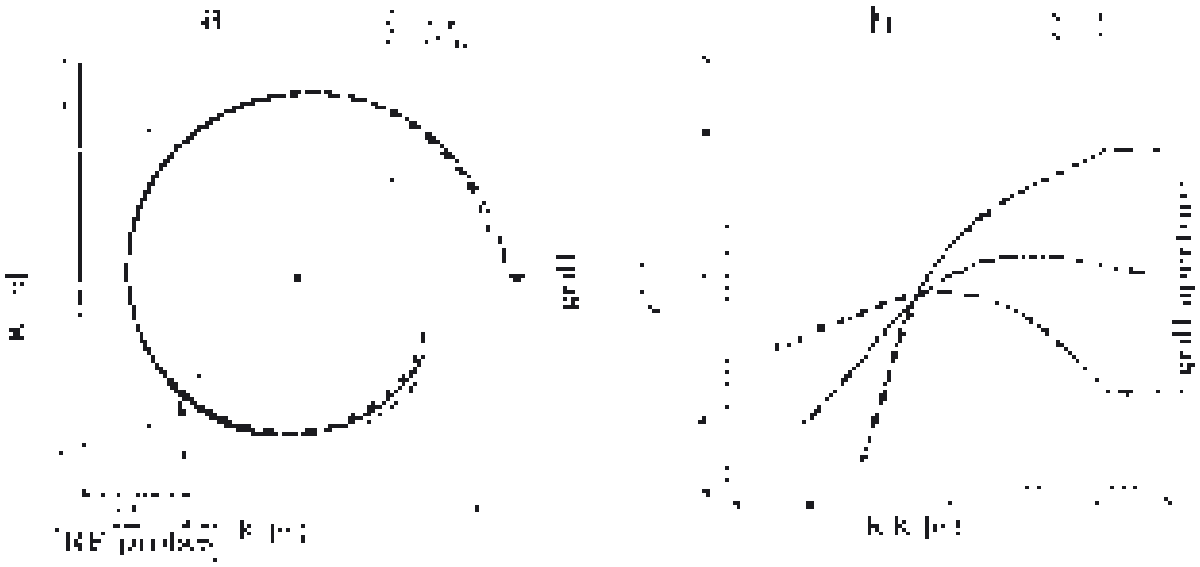

(a) **(b)**

Fig. 1. Ray tracing of LHW with $f = 1.25\,\mathrm{GHz}$ launched near CASTOR equatorial plane for a parabolic density distribution with $n(0) = 7\times10^{18}\,\mathrm{m}^{-3}$ ($\bar{n} \doteq 4 \times 10^{18}\,\mathrm{m}^{-3}$, see Fig. 4); (a) top view; (b) poloidal cross section.

(b) the dependence of the power reflected back into the launching antenna on the density of plasma in front of the quasi-optical grill [3] matches very well that predicted by the theory of LHW coupling [4].

However, strong fluctuations of LHW amplitude and phase observed during all these measurements precluded the determination of the wave $N_{||}$, and the main goal of this work could not be reached.

Motivation of this work is a natural question arising in this situation: are these fluctuations specific for the quasi-optical grills, or do they accompany LHW launched by other types of grills, too? We attempted to answer this question by repeating the experiments with a multijunction grill working at the frequency $f = 1.25\,\mathrm{GHz}$ and a power up to 50 kW, sufficient for a substantial current drive [6]. Results of these experiments are presented in this paper. A short description of the experiment on the CASTOR tokamak is given in Section II. Section III presents the experimental results obtained and, in Section IV, these results are interpreted. We emphasize that the interpretation does not concern the reason for spectral broadening of the launched LHW spectrum [7]–[10]. This effect is asumed here as a (commonly used) hypothesis and it is shown that it implies results which are consistent with the data obtained in the experiment described below.

II. Experimental Arrangement

CASTOR is a small limiter tokamak with the following parameters: major radius, $R = 0.4\,\mathrm{m}$; wall radius, $b = 0.1\,\mathrm{m}$; limiter radius, $a = 0.085\,\mathrm{m}$; magnetic field on

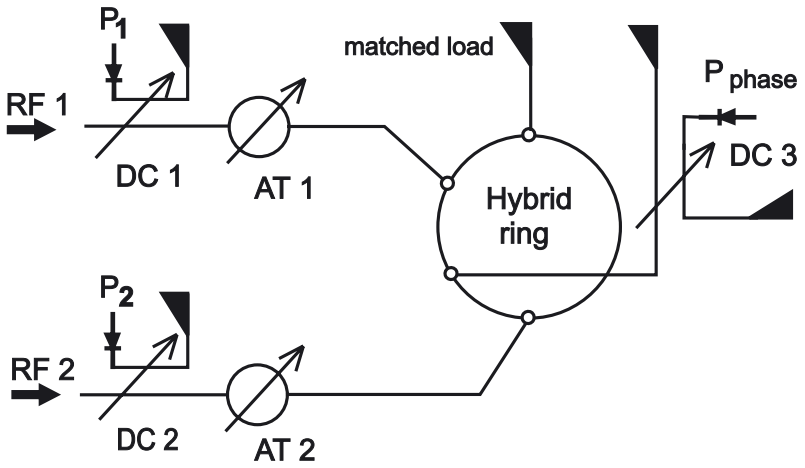

Fig. 2. RF coaxial circuit for detection of the LHW phase velocity.

the axis, $B(0) \leq 1.5\,\mathrm{T}$; plasma density on the axis, $n(0) \leq 3 \cdot 10^{19}\mathrm{m}^{-3}$; length of the discharge, $\tau \leq 40\,\mathrm{ms}$.

To facilitate finding the best position for direct measurement of LHW inside the chamber of the CASTOR tokamak, ray-tracing computations were performed for a frequency $1.25\,\mathrm{GHz}$ and for the stationary phase of a chosen CASTOR regime: $n_\mathrm{e}(0) = 7 \times 10^{18}\,\mathrm{m}^{-3}$, $T_\mathrm{e}(0) = 170\,\mathrm{eV}$, $I_\mathrm{p} = 8\,\mathrm{kA}$, $B_\mathrm{T}(0) = 1\,\mathrm{T}$. Before giving results of such computations, a comparison of the relevant wavelengths and plasma dimensions is necessary. Taking $N_\parallel \simeq 2$ for the largest characteristic wavelength and $n_\mathrm{e} \simeq 4 \times 10^{18}\,\mathrm{m}^{-3}$, we have the LHW wavelengths parallel ($\lambda_\parallel$) and perpendicular ($\lambda_\perp$) to the magnetic field, $\lambda_\parallel \simeq 12\,\mathrm{cm} \ll \pi R \simeq 120\,\mathrm{cm}$, and $\lambda_\perp \simeq 0.8\,\mathrm{cm} \ll a \simeq 8\,\mathrm{cm}$. The last two inequalities provide information on the applicability of the ray-tracing code here. Due to the massive current drive (see Section III), the waves are damped and, therefore, a radial mode structure is not likely to occur.

An example of the ray-tracing computation is given in Fig. 1. Fig. 1(a) (top view) shows the rays of LHW outgoing from the centre (the initial vertical coordinate of the ray $z = 0$, see Fig. 1(b)), and from the upper ($z = +5\,\mathrm{cm}$) and lower ($z = -5\,\mathrm{cm}$) parts of the grill aperture for $N_\parallel = 4$. Fig. 1(b) shows the projection of the same rays (however, in this case for $N_\parallel = 4$ and 6) in the poloidal cross section of the CASTOR tokamak. It is seen (on the right-hand side of Fig. 1(b)) that the launching antenna is placed in the low-field-side port and its poloidal shape is aligned to the plasma column cross section. The ray-tracing computation has been made for a parabolic plasma density profile with central value $n(0) = 7 \times 10^{18}\,\mathrm{m}^{-3}$. Obviously, the rays depend only weakly on the $N_\parallel$ value.

For the measurement of the LHW $N_\parallel$ spectrum, a double RF coaxial probe with two measuring tips 1 and 2, placed in a poloidal cross section 225° toroidally away from the grill antenna (see Fig. 1(a)), has been used. Receiving tips 1 and 2 of the probe are a distant 6 mm toroidally from each other (the distance of 6 mm corresponds to the phase difference $\varphi \simeq 90^\circ$ if a slowed wave with $N_\parallel \doteq 10$ is

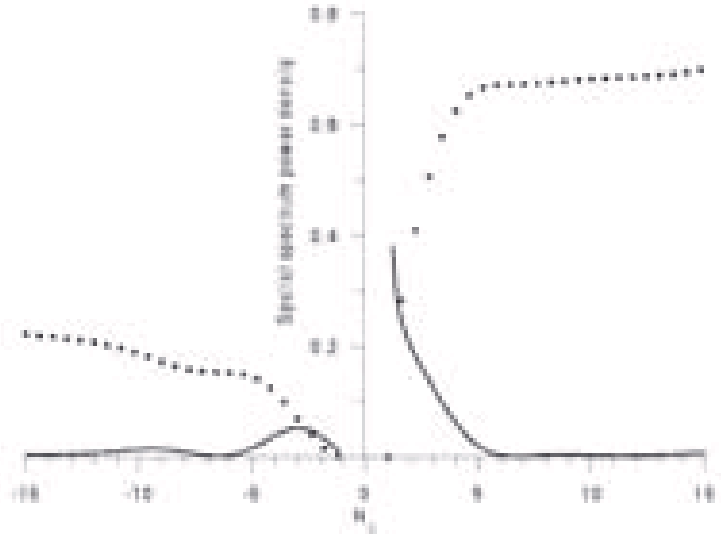

Fig. 3. The three-waveguide multijunction grill (used in the experiment) power spectrum, computed for the plasma density $n = 1 \times 10^{18}\,\mathrm{m}^{-3}$ and radial density gradient $\nabla n = 10^{20}\,\mathrm{m}^{-4}$ at the grill mouth; dotted curves are integrated spectral power densities.

supposed). The tips have a length of $5\,\mathrm{mm}$ and they are oriented in the supposed direction of the LHW electric field $\vec{E}$, i.e. nearly radially. The probe enters the plasma through a lower port and it is movable through the whole poloidal cross section of the device.

A coaxial RF interferometric circuit for determination of the wave phase velocity (i.e. the mutual phase φ of the wave at two tips 1 and 2) for the case of a rapidly changing wave amplitude has been developed and assembled, see Fig. 2. RF1 and RF2 in the figure denote the feeding coaxial lines from the two RF tips 1 and 2, DC are variable directional couplers for measurement of RF powers (squares of wave electric field) and AT are attenuators. A hybrid ring junction has been used as a mixer for the phase measurement. Each of the three detecting diodes shown in Fig. 2 is absolutely calibrated in the whole range of the power used (to exclude any differences in the characteristics and departures from the quadratic dependences of output voltages P_1, P_2, and P_{ph} on the corresponding wave electric fields).

For the absolute phase measurements, the difference in electrical lengths of both the coaxial RF lines 1 and 2 from the respective RF tips 1 and 2 to the mixer has been determined on the test stand. For this purpose a synphase feeding of both RF tips at a frequency $f = 1.25\,\mathrm{GHz}$ has been assured. Using a high-sensitivity phase device (HP Network Analyser 8410B), the line 1 has been found to be $10^\circ \pm 1^\circ$ longer.

The data measured have been stored using a transient recorder with sampling rate of up to $5\,\mathrm{MS/s}$, a resolution of $12\,\mathrm{bits}$ and memory of up to $128\,\mathrm{kB/channel}$.

For evaluation of the mutual phase φ between the fast fluctuating RF signals P_1 and P_2, the interferometric scheme shown in Fig. 2 has been adjusted (in the

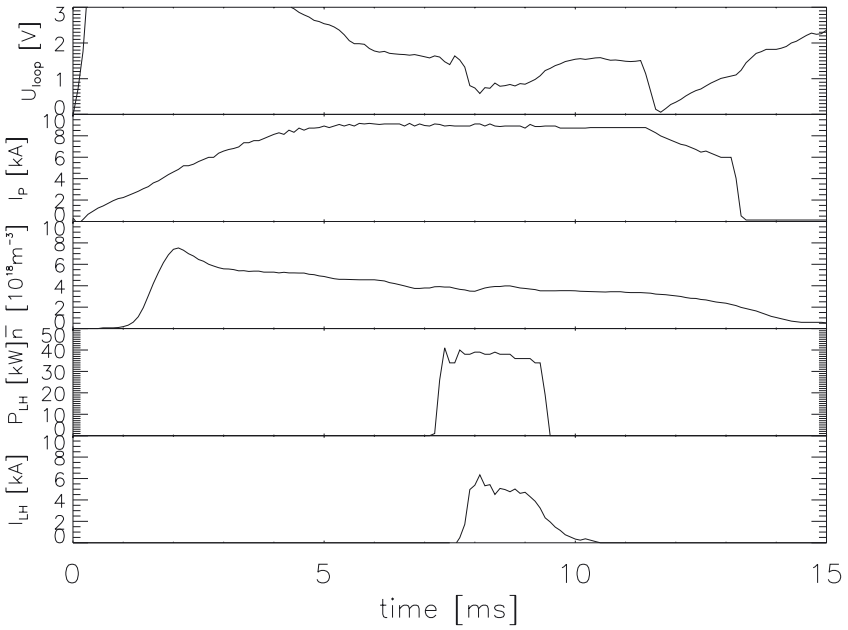

Fig. 4. Loop voltage $U_{\rm loop}$, plasma current $I_{\rm p}$, line-averaged plasma density $\bar{n}$, incident LH power $P_{\rm LH}$ and noninductively generated LH current $I_{\rm LH}$ in a typical CASTOR discharge with LHCD (shot #5581).

absence of the plasma) in the following way:

1) $P_1 \equiv P_{\rm ph}$ for AT2 = max (closing of the second arm of the interferometer),
2) $P_2 \equiv P_{\rm ph}$ for AT1 = max (closing of the first arm of the interferometer).

After opening of both interferometric arms, the phase φ can be determined in the following form:

$$\varphi = \arccos \frac{P_{\rm ph} - (P_1 + P_2)}{2 \cdot \sqrt{P_1 \cdot P_2}}.$$

As a launcher, a three-waveguide multijunction grill (having the phase shift between adjacent waveguides 90°) with a relatively broad spectrum $1 \leq N_{\|} \leq 5$ has been used (the output dimensions of the grill mouth are 160 mm in the poloidal and 50 mm in the toroidal directions). The spectral power density of the waves launched by this grill, computed theoretically for the edge plasma density $n = 1 \times 10^{18}\,{\rm m}^{-3}$ and a radial gradient $\nabla n = 10^{20}\,{\rm m}^{-4}$ at the grill mouth, is given in Fig. 3. The power of the RF generator used (several tens of kW) is comparable with the ohmic heating power.

III. Experimental Results

A typical discharge of the CASTOR tokamak in the lower hybrid current drive (LHCD) regime is shown in Fig. 4, where loop voltage $U_{\rm loop}$, plasma current $I_{\rm p}$, line-averaged density $\bar{n}$ measured by 4 mm microwave interferometer, and LHW incident power $P_{\rm inc}$ are given. The last trace is the value of the non-inductive